DA-07-056

Applying the Effectiveness-NTU Method to Elemental Heat Exchanger Models

Ipseng Iu
Student Member ASHRAE

N.A. Weber
Associate Member ASHRAE

Pradeep Bansal, PhD
Member ASHRAE

D.E. Fisher, PhD
Member ASHRAE

ABSTRACT

Elemental heat exchanger models are increasingly used in heat pump design calculations because of their ability to accurately model complex heat exchanger circuits and non-uniform coil face velocities. These models usually assume that refrigerant properties are constant in each element. For transition elements, where both single-phase and two-phase refrigerant are present, this assumption introduces some error in the capacity calculation and, more importantly, results in dual-valued property functions that may trap the numerical solver at an unconverged point in the solution domain. This paper illustrates both the capacity error and the numerical error that can result from improper handling of the transition element in an elemental heat exchanger model. An algorithm that correctly handles the transition element is proposed. Examples are presented to illustrate improvements in the capacity calculation and the simulation performance due to the proposed algorithm. The proposed algorithm is specifically applied to the ε-NTU heat exchanger calculation method but can also be applied to the LMTD method without loss of generality.

INTRODUCTION

The heat exchanger model is an important aspect of the overall design and simulation of the air-to-air heat pump. There are many convergence criteria in the system design and simulation program that are closely related to the outputs of the heat exchanger model. This paper presents the results of coupling the ORNL heat pump solver (Fischer et al. 1998) with an elemental heat exchanger model (Ragazzi and Pedersen 1991). A straightforward coupling of the solver with the heat exchanger model without special consideration of the transition elements, which model the transition from single-phase to two-phase flow and vice-versa, was unsuccessful. Converged solutions could violate the first law of thermodynamics, and unconverged solutions were common. This paper reviews the algorithmic and numeric problems that result from a straightforward coupling of the solver with the elemental heat exchanger model and presents an algorithm that solves both the thermodynamic and numeric errors.

Heat exchanger models commonly used in heat pump design calculations can be classified by their calculation domains. The zone-by-zone method (Fischer et al. 1998; Heun and Dunn 1996; Mullen et al. 1998; Shah et al. 2004) divides the heat exchanger into zones according to the state of the refrigerant. For example, a condenser has no more than three refrigerant zones: superheated, two-phase, and subcooled. Orth et al. (1995) developed a heat exchanger model that first divides the heat exchanger into zones and then subdivides the two-phase zone into small segments to enhance modeling accuracy. However, their model is limited by simple heat exchanger circuits, and the circuiting effect in the single-phase zones is ignored. The zone-by-zone method is computationally efficient but is unable to completely capture the effects of heat exchanger circuiting that can alter the heat exchanger capacity and pressure drop (Ellison et al. 1981; Liang et al. 2001; Iu et al. 2003). If the heat exchanger calculation proceeds along the refrigerant flow path in the heat exchanger, the circuiting effect can be captured automatically in the calculation.

The general elemental method divides the heat exchanger tubes into small elements. The elements can be as long as a single tube (Ellison et al. 1981; Liang et al. 2001; Domanski and Didion 1983) or as small as a small segment of a tube (Kim and Bullard 2001; Jiang et al. 2002; Ragazzi and Pedersen

Ipseng Iu is a graduate student and **D.E. Fisher** is associate professor in the Department of Mechanical and Aerospace Engineering, Oklahoma State University, Stillwater, OK. **N.A. Weber** is senior design engineer in the Department of Engineering, York International Unitary Products Group (a Johnson Controls Company), Norman, OK. **Pradeep Bansal** is associate professor in the Department of Mechanical Engineering, University of Auckland, Auckland, New Zealand.

1991; Vardhan and Dhar 1998). Each element is treated as a single-tube heat exchanger and is calculated one by one along the refrigerant flow direction. The local boundary conditions of each element are obtained from the surrounding element calculations. Elemental methods can capture not only the effect of the circuiting but also the effect of nonuniform air distribution entering the heat exchanger. Air maldistribution has a significant impact on the heat exchanger capacity, as shown in Domanski (1991), but the zone-by-zone methods are not able to calculate its effects. The downside of the elemental method is that it is computationally intensive because of the elemental calculation procedures. However, it is still widely used in heat exchanger modeling because of its modeling capabilities and accuracy.

No matter what discretization is applied to the heat exchanger, the same heat exchanger calculations can be applied to each calculation domain. The log-mean-temperature-difference (LMTD) and effectiveness-NTU (ε-NTU) methods are two commonly used heat exchanger calculation procedures. The LMTD method calculates heat exchanger capacity as follows:

$$\dot{Q} = UAF(\text{LMTD}) \tag{1}$$

where

$$\text{LMTD} = \frac{\Delta T_{in} - \Delta T_{out}}{\ln(\Delta T_{in} / \Delta T_{out})} \ . \tag{2}$$

For counterflow heat exchangers, the correction factor (F) is unity. For other flow configurations, it can be obtained from the correction factor plot presented in Incropera and DeWitt (1996). Note that the capacity is correlated to both the inlet and outlet temperatures. It is sometimes inconvenient to use when the outlet temperature is unknown and iteration is needed for the capacity calculation. Compared to the LMTD method, the ε-NTU method is a feed-forward procedure that does not require knowledge of the outlet temperature to calculate capacity. Capacity is defined as

$$\dot{Q} = \varepsilon \cdot C_{min}(T_{h,in} - T_{c,in}) \ . \tag{3}$$

The ε-NTU method is used in many elemental heat exchanger models (Ellison et al. 1981; Iu et al. 2003; Ragazzi and Pedersen 1991; Vardhan and Dhar 1998; Liaw et al. 2002; Harms et al. 2004). However, the potential problems of using the ε-NTU method and the elemental heat exchanger model are not addressed. Such problems may result in the violation of the first law of thermodynamics and unconverged numeric solutions. This paper addresses the sources of these potential problems and proposes a correction algorithm to be used with the ε-NTU method in elemental heat exchanger models.

BACKGROUND

The potential problems of using the ε-NTU method in elemental heat exchanger models occur at the transition element (a tube or a segment) where both single-phase and two-phase refrigerants exist. Note that zone-by-zone-based heat exchanger models do not have this problem because each zone can only have either single-phase or two-phase refrigerant. But, as mentioned before, zone-by-zone models have limitations in handling heat exchanger circuiting that can be overcome by elemental models. However, the transition element problems in elemental models have not been adequately addressed in the literature. Because the calculation sequence in the elemental heat exchanger model is along the refrigerant flow path, it is possible for a heat exchanger element to have a two-phase inlet condition but a single-phase outlet condition for evaporation and vice versa for condensation. However, elemental heat exchanger models assume that the refrigerant properties are constant for the entire element. The refrigerant property used to determine the heat transfer calculations is usually the inlet property or the average property across the element. The representative refrigerant property determines whether the single- or two-phase correlation should be used in the heat transfer calculations. Misuse of the correlations can result in overpredicting or underpredicting capacity. Although this error is usually small (depending on the number and relative size of the transition element), significant numerical errors can be introduced as a result of improperly calculating properties for the transition element. In the ε-NTU method, there are two instances where a single-phase or two-phase equation must be chosen according to the refrigerant state: (1) the effectiveness (ε) equation and (2) the refrigerant-side heat transfer coefficient (h_{ref}) correlation.

Application of the Effectiveness Equation to the Transition Element

Effectiveness is calculated using the following equations (Incropera and DeWitt 1996). For single phase:

If C_{min} is unmixed and C_{max} is mixed,

$$\varepsilon_{SP} = \frac{1}{C_r}(1 - \exp\{-C_r[1 - \exp(-\text{NTU})]\}) \ . \tag{4}$$

If C_{min} is mixed and C_{max} is unmixed,

$$\varepsilon_{SP} = 1 - \exp\left\{-\frac{1}{C_r}[1 - \exp(-C_r \cdot \text{NTU})]\right\} \ . \tag{5}$$

If both C_{min} and C_{max} are unmixed,

$$\varepsilon_{SP} = 1 - \exp\left\{-\frac{1}{C_r}NTU^{0.22}[\exp(-C_r \cdot \text{NTU}^{0.78})]\right\} \ . \tag{6}$$

The unmixed or mixed state of the fluid is determined by the geometry of the fluid flow passages (Kakac and Liu 2002). Flow through a louvered fin heat exchanger is considered mixed since the perforated surface of the louvered fin accommodates cross-mixing of the flow paths. Flow through nonperforated fin heat exchangers is considered unmixed since there is no mechanism for mixing. On the refrigerant

side, the refrigerant is always considered unmixed in the segment-by-segment calculation. The unmixed C_{min} and C_{max} equation is more suitable for heat exchangers with smooth fins.

For two-phase,

$$\varepsilon_{TP} = 1 - \exp(-\text{NTU}), \quad (7)$$

where

$$C_r = C_{min}/C_{max} \text{ and} \quad (8)$$

$$\text{NTU} = UA/C_{min}. \quad (9)$$

The single-phase and two-phase effectivenesses differ in magnitude. Figure 1 shows the change of effectiveness with heat capacity ratio at NTU = 3.5. Note that ε_{TP} is greater than ε_{SP} and is constant because it is independent of C_r. All cases of ε_{SP} approach ε_{TP} when C_r goes to zero. Although Figure 1 only compares ε_{SP} and ε_{TP} for a specific NTU value, ε_{TP} is always greater than ε_{SP} in the physical range of NTU values. This implies that if ε_{TP} is used for the transition element, the capacity will be overpredicted. But if ε_{SP} is used, the capacity will be underpredicted, as shown in Figure 1.

Application of Refrigerant-Side Heat Transfer Coefficient to the Transition Element

Selection of a refrigerant-side heat transfer correlation presents a similar problem in the transition element. The refrigerant-side heat transfer coefficient affects the *UA* value of the element. Neglecting fouling and contact resistances, the *UA* value is defined as

$$\frac{1}{UA} = \frac{1}{h_{ref} A_{ref}} + R_{tube} + \frac{1}{\eta_s h_{air} A_{air}}, \quad (10)$$

where

$$\eta_s = 1 - \frac{A_{fin}}{A_{air}}(1 - \eta_{fin}). \quad (11)$$

Incropera and DeWitt (1996) show that the two-phase heat transfer coefficient is higher than the single-phase, especially in the high-quality region. A higher h_{ref} results in a higher *UA* and ultimately a higher NTU. Figure 2 shows the changes of ε with NTU at $C_r = 0.5$. Note that ε increases with increasing NTU. This trend also exists for other C_r values because of the relationship of NTU and h_{ref} (Equations 9 and 10). Therefore, the element capacity will be overpredicted if the two-phase h_{ref} is used in the transition element.

Figure 2 also illustrates the combined effect of the effectiveness equation and the heat transfer coefficient on the resulting effectiveness. Note that ε increases rapidly for small NTU values where ε_{SP} and ε_{TP} are similar. That is, the heat transfer coefficient dominates when NTU is small. As NTU increases, ε is more sensitive to the effectiveness equations than the NTU and heat transfer coefficient equations. The effectiveness equation dominates when NTU is large. Note that this trend only exists when C_r is not close to zero since ε_{SP} approaches ε_{TP} as C_r approaches zero, as shown in Figure 1. A zero heat capacity ratio means that either air or refrigerant is not moving at all, which rarely happens in heat pump applications. Therefore, in general, the effect of the heat transfer coefficient dominates in the low-NTU range, and the effectiveness equation has an increasing effect as NTU increases.

The transition element problem also exists in the LMTD method. It also involves the *UA* calculation that is related to the selection of the refrigerant-side heat transfer coefficient. However, the combined effect of the effectiveness equation and the heat transfer coefficient makes the transition problem more noticeable and significant in the ε-NTU method.

THERMODYNAMIC AND NUMERIC ERRORS

Improper modeling of the transition element can result in both thermodynamic inconsistencies and unconverged solutions in the heat pump simulation. In system design calculations, one of the heat exchanger boundary conditions is adjusted per iteration to match the specified rating conditions

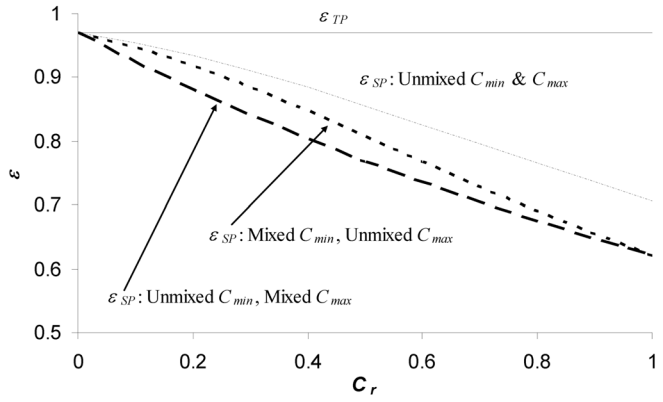

Figure 1 *Effectiveness vs. heat capacity ratio for NTU = 3.5.*

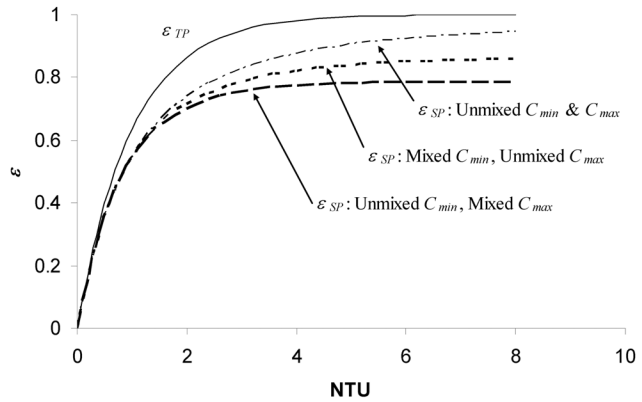

Figure 2 *Effectiveness vs. NTU for* $C_r = 0.5$.

(Fischer et al. 1998). For the high-pressure-side calculation, the condenser saturation temperature is adjusted to find a match in calculated and specified subcooling levels. It is important that the calculated subcooling respond to the adjusted saturation temperature in a thermodynamically realistic and consistent manner. If the saturation temperature is increased, because of a higher temperature gradient between the air and refrigerant, the condenser capacity should increase, as should the resulting subcooling. This consistent trend is key for the numerical solver to adjust the boundary conditions properly and converge on a correct solution.

The convergence problem can be illustrated by considering a single-circuit heat exchanger that has 12 tubes with 6 tubes per row (Figure 3). The tubes are connected with U-bends and configured to a counter-cross-flow circuitry. Louver fins are used on this heat exchanger. Detailed physical dimensions of the heat exchanger are listed in Table 1. The heat exchanger was simulated as a condenser with a tube-by-tube discretization. For each tube, the average refrigerant property was used to define the refrigerant phase for the entire tube. Table 2 shows the correlations used in the heat exchanger calculation. Note that the evaporation heat transfer correlation is used later in an evaporator simulation example. The boundary conditions for the condenser simulation were:

$T_{air,in}$ = 35°C, $\phi_{air,in}$ = 41%, $\dot{V}_{air}$ = 56.4 m^3/min
$T_{ref,in}$ = 78°C, $\dot{m}_{ref}$ = 52 kg/h
Refrigerant = R-22

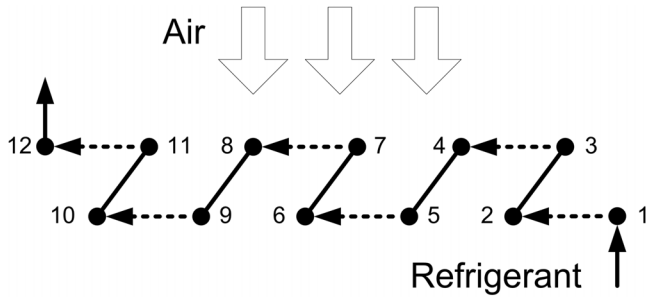

Figure 3 *Sample heat exchanger (hidden lines represent the invisible side).*

Inlet refrigerant pressure varied from 1395.6 to 1613.5 kPa, which is equivalent to the variation of saturation temperature from 37.7°C to 42.8°C. Figure 4 shows the subcooling or quality at the condenser outlet corresponding to the variation of saturation temperature. Quality decreases with increasing saturation temperature, as expected. However, there is a problem near the two-phase subcooled outlet conditions, where the subcooling is inconsistently higher than the neighboring point. This violates the first law, as previously mentioned, and creates problems for the numerical solver in the system design calculations. When the solver encounters a local minimum in the subcooling during the iteration process, it will likely fail to converge on the saturation temperature that matches the specified subcooling.

Figure 5 shows the accumulated capacity from tube to tube for the three data points near zero quality. The figure shows that the capacity increases as more tubes are taken into account in the calculation. The accumulated capacity is higher at higher saturation temperatures up to the 11th tube. Note that at tube 12, the capacity is the highest at T_{sat} = 39.6°C, even higher than the capacity at T_{sat} = 39.9°C. Although the capacity difference is only about 1%, it violates the first law because of the transition element problem. More importantly, it creates a trap for the numerical solver in the system design calculation, which could lead to an unconverged solution, and the simulation result would become dubious. At T_{sat} = 39.6°C, tube 12 is a transition tube, but it is a single-phase tube at T_{sat} = 39.9°C. Because the average refrigerant property at tube 12 is two-phase, the two-phase equations were used for T_{sat} = 39.6°C, and the capacity was overpredicted.

Table 1. Heat Exchanger Physical Dimensions

Heat Exchanger Parameters	Dimensions
Single tube length	1.5 m
Tube outside diameter	9.5 mm
Tube wall thickness	0.3 mm
Row spacing (parallel to the airflow direction)	22.0 mm
Tube spacing (normal to the airflow direction)	25.4 mm
Fin pitch	6 fins per cm
Fin thickness	0.1 mm
Louver height	0.9 mm
Louver spacing	1.5 mm

Table 2. Heat Transfer and Pressure Correlations for Heat Exchanger Calculations

Air-Side Calculations		Refrigerant-Side Calculations				
		Heat transfer coefficient				
Heat transfer coefficient	Fin efficiency	Single-phase	Two-phase condensation	Two-phase evaporation	Pressure drop	Return bend pressure drop
Wang et al. (1999)	Schmidt (1949)	Gnielinski (1976)	Dobson (1994)	Wattelet (1990)	Souza et al. (1993)	Paliwoda (1992)

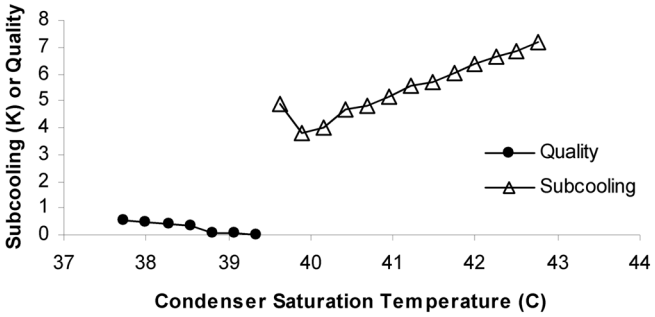

Figure 4 *Condenser simulation with elemental heat exchanger model.*

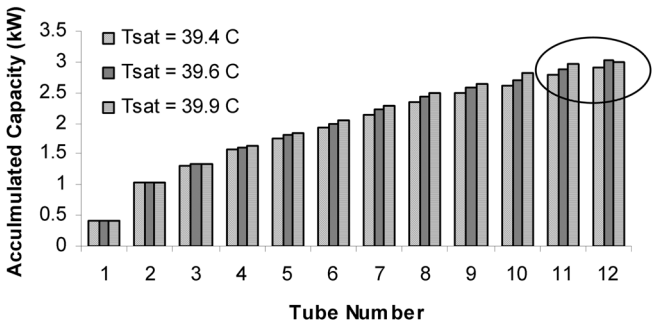

Figure 5 *Accumulated capacity; the circle indicates the transition element problem.*

Another potential convergence problem is at the low-pressure-side iteration. In the heat pump design calculation, the evaporator superheat is specified, and the iteration adjusts the entering air temperature to the evaporator until the calculated superheat matches the specified value (Fischer et al. 1998). Therefore, it is necessary for the evaporator model to respond correctly to the change of air temperature to find a converged solution. For the same heat exchanger used in the condenser simulation (Figure 3 and Table 1), a tube-by-tube evaporator was simulated using the air- and refrigerant-side correlations in Table 2. The following boundary conditions were applied to the simulation:

$\phi_{air,in}$ = 52%, $\dot{V}_{air}$ = 34.2 m^3/min
$T_{ref,in}$ = 11.9°C, $P_{ref,in}$ = 720 kPa, $\dot{m}_{ref}$ = 52 kg/h
Refrigerant = R-22

The entering air temperature varied from 12.5°C to 22°C. As in the condenser simulation, the average refrigerant property was used to define the refrigerant phase in each tube. The evaporator was simulated with a dry surface, with no dehumidification occurring. Figure 6 shows the evaporator outlet quality or superheat corresponding to the change of entering dry-bulb air temperature. Note that the transition tube problem appears when the entering air temperature is high enough to cause superheated refrigerant at the evaporator outlet. The evaporator superheat does not increase with increasing entering air temperature consistently. For example, at $T_{air,in}$ = 18.5°C, the superheat is higher than at $T_{air,in}$ = 19°C. This is due to the misuse of the heat transfer coefficient and the effectiveness equations, which overpredicts capacity in the transition element. If the numerical solver encounters this superheat output curve in the system design calculations, it will fail to converge.

The required calculation time for elemental heat exchanger models is a major concern in heat pump design calculations. If the transition element problem occurs in both the condenser and evaporator calculations, either the solver will fail to converge or the number of iterations in the numerical solver will increase and the overall calculation time will be significantly longer. Therefore, it is necessary to have a

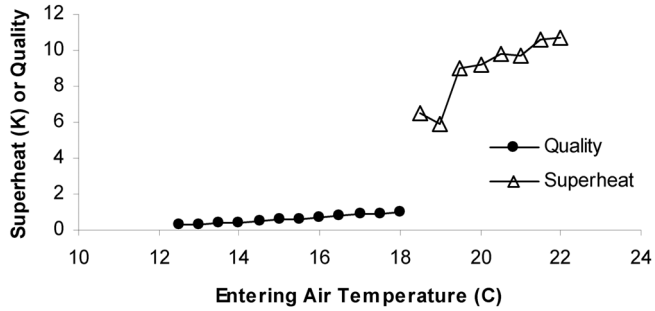

Figure 6 *Evaporator simulation with elemental heat exchanger model.*

solution to handle the transition element problem such that the elemental heat exchanger models can produce realistic results for heat pump design calculations.

Although the above simulation examples are based on tube-by-tube discretization, a finer segment-by-segment discretization can reduce the impact of the transition element problems. However, the intrinsic problems of the transition element still exist. A small tube segment can still have both single-phase and two-phase refrigerants, and choosing the correct equations to use can still be problematic. In addition, segment-by-segment simulations require even more computational time than the tube-by-tube simulations, and it is hard to determine how many segments should be used in the simulation to minimize the effect of transition element problems. Therefore, regardless of whether tube-by-tube or segment-by-segment discretization is used in elemental heat exchanger models, the transition element problems still exist and must be remedied. The following section introduces an algorithm that can eliminate transition element problems.

PROPOSED SOLUTION ALGORITHM

The root of the transition element problems is the constant refrigerant property assumption in the elemental heat exchanger models. When the transition element is encountered in the heat exchanger calculation, it is difficult to

choose the representative equations to use for the entire element. If only the single-phase equations are used, the capacity will be underpredicted; if only two-phase equations are used, the capacity will be overpredicted. To accurately calculate the transition element capacity, it is necessary to subdivide the element into single-phase and two-phase portions. As a result, the constant property assumption should not apply to the entire transition element.

If the boundary between the single-phase and two-phase regions is known in the transition element, it is possible to apply the appropriate heat transfer equations in each portion. Hence, the element capacity is the combined capacities from the single-phase and two-phase portions. Because the refrigerant property is known at the element inlet, it is possible to calculate the capacity for the first portion using the available enthalpy difference. The capacity is calculated differently depending on the location of the transition element; for the transition elements near the condenser inlet, the first portion of the refrigerant is single-phase and its capacity is

$$\dot{Q}_1 = \dot{m}(i_{ref,in} - i_{ref,vap}) \ . \quad (12)$$

Similarly, the capacity of the transition elements near the condenser outlet is

$$\dot{Q}_1 = \dot{m}(i_{ref,in} - i_{ref,liq}) \quad (13)$$

and the capacity of the transition element near the evaporator outlet is

$$\dot{Q}_1 = \dot{m}(i_{ref,vap} - i_{ref,in}) \ . \quad (14)$$

Knowing transition element capacity in one portion allows us to find the boundary between the single-phase and two-phase regions and, consequently, the capacity in each portion. Figure 7 shows the algorithm to simulate transition elements. The procedures are summarized as follows:

1. Assume constant refrigerant property in the entire element and apply either single- or two-phase heat transfer equations to calculate capacity.
2. Compare refrigerant properties at the element inlet and outlet to check for a refrigerant phase change. If there is no phase change, it is not a transition element. Otherwise, check whether the transition element is located either near the condenser inlet, condenser outlet, or evaporator outlet.
3. Calculate the capacity for the first part of the element using Equation 12, 13, or 14 according to the element location.
4. Guess the length of the first portion. It should be between zero and the total element length.
5. Compute the first portion capacity using the ε-NTU method. If the element is near the condenser inlet, use the single-phase heat transfer equations. Otherwise, use the two-phase equations.
6. Compare the capacities calculated at steps 3 and 5. If they do not match, adjust the guessed length and repeat step 5. Note that the length is proportional to the capacity and is bounded. Therefore, it is well suited for any one-dimensional search method.
7. Subtract the length of the first part from the total element length to obtain the second portion length.
8. Compute the capacity for the second part. If the element is near the condenser inlet, use the two-phase equations. Otherwise, use the single-phase equations.
9. Add the capacities of the first and second parts from steps 5 and 8, respectively. The result is the total capacity of the transition element.

Once the transition boundary is located, we can apply the appropriate effectiveness equation and heat transfer coefficient for the respective single- and two-phase element portions. Potential problems due to the misuse of the heat transfer coefficient and the effectiveness equations are automatically eliminated.

It may take extra computational time to find the transition boundary in the proposed algorithm. But if it can correct the heat exchanger model to produce realistic results and lead to the converged solution, it is worthwhile to spend a little more time finding the transition boundary rather than doing a number of iterations that might not get to the converged solution.

Although the proposed algorithm is designed for the ε-NTU method, it is also applicable to the LMTD method without a loss of generality. The LMTD method may also experience the transition element problem but with the sole effect of the refrigerant-side heat transfer coefficient. If the proposed algorithm is used in the LMTD method, the calculation of the effectiveness is not necessary, and Equation 3 should be replaced by Equation 1 in the algorithm.

EVALUATION

The transition element algorithm was implemented in an elemental heat exchanger model. The updated heat exchanger model was evaluated with the same aforementioned examples. The same boundary conditions and discretization (i.e., tube-by-tube) were used to run the heat exchanger simulations. Figures 8 and 9 show the new simulation results for the condenser and evaporator, respectively. Note that the old simulation results that did not use the transition element algorithm are also presented for comparison. Compared to the old simulation results, the results with the transition element algorithm are more reasonable. The transition element problems are eliminated in the new simulation results and the simulations respond to the change of boundary conditions realistically.

Note in Figure 8 that the new simulation result predicted subcooled refrigerant at the condenser outlet when the saturation temperature is above 40.2°C. However, the old result shows that subcooled refrigerant exists when the saturation temperature is above 39.4°C. This implies that the heat exchanger simulation without the transition element algorithm

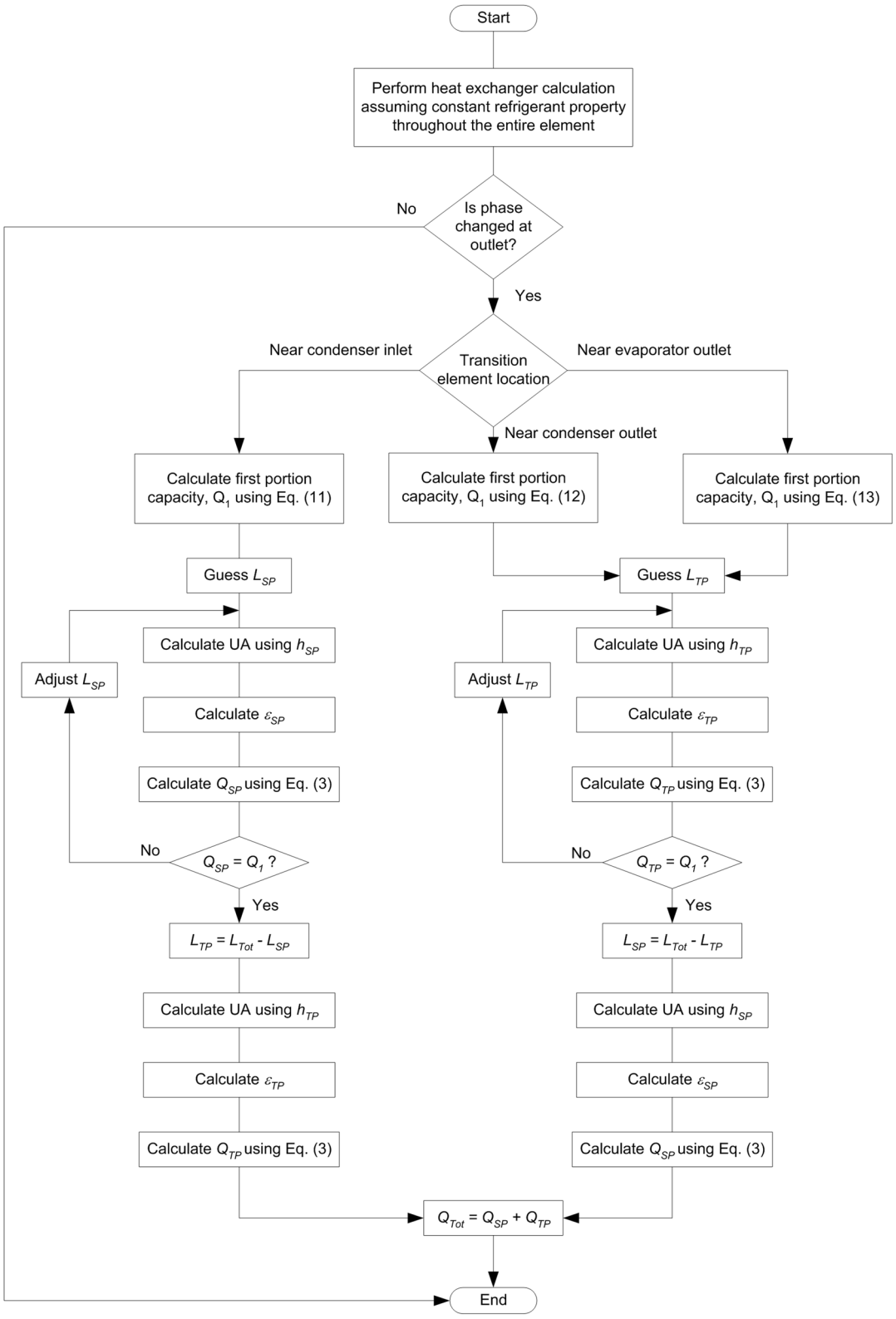

Figure 7 *Transition element solution algorithm.*

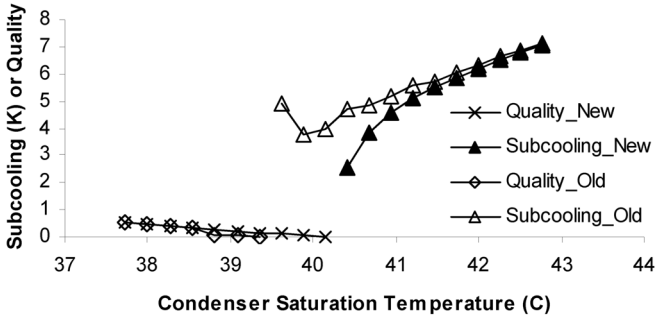

Figure 8 *Comparison of condenser simulations with (new) and without (old) transition element algorithm.*

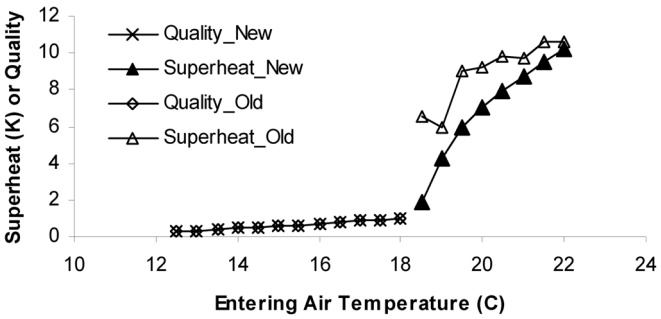

Figure 9 *Comparison of evaporator simulation with (new) and without (old) transition element algorithm.*

predicted higher capacity. If there is no subcooled refrigerant, the transition element near the condenser outlet does not exist. However, the transition element near the condenser inlet still contributes problems to the heat exchanger simulation. Because the average refrigerant property was used as a representative value in each element, the element capacity was overpredicted even though the first part of the element is single-phase refrigerant. As a result, subcooled refrigerant exists at a lower saturation temperature. If the inlet refrigerant property were used, the element capacity would be underpredicted, and the condenser subcooling would appear at a higher saturation temperature than that shown in Figure 8.

Figure 8 also shows that the new and old simulation results become similar when there is more subcooled refrigerant. As the saturation temperature increases, one of the refrigerant phases in the transition element becomes dominant and the transition element effect fades out. Although the simulation without the transition element algorithm is able to predict reasonable results for high subcooling conditions, it could cause convergence problems in heat pump design calculations when the iteration projects a low subcooled outlet condition. The simulation with the transition element algorithm eliminates this problem.

The evaporator simulation results are compared in Figure 9. After the transition element problems are corrected, the evaporator model responds to the change of air temperature reasonably. Evaporator superheat increases with increasing entering air temperature. Note that when there is only two-phase refrigerant in the evaporator, the simulated qualities are the same for both new and old simulations. Unlike the condenser simulation where there are two possible transition elements near the condenser inlet and outlet, the only possible transition element in this evaporator is near the evaporator outlet. But if the entering air temperature is not high enough to produce superheated refrigerant at the evaporator outlet, no transition elements occur in the simulation and both simulation results are identical.

As the air temperature increases, the single- to two-phase refrigerant ratio in the transition element changes. The transition element effect varies according to the refrigerant ratio, as shown in Figure 9. It is least significant when one of the refrigerant phases dominates. Similar to the condenser simulation, both the old and new simulation results approach each other when there is more superheated refrigerant in the evaporator. For the same reason, when one refrigerant phase dominates in the transition element, the simulation result is similar to that with the transition element algorithm.

The transition element algorithm shows a significant improvement in elemental heat exchanger models when there is a transition element in the simulations. It corrects the model output response to the change in boundary conditions. The correct response is very important in heat pump design calculations where the numerical solver uses the model outputs to adjust the iteration parameter.

CONCLUSIONS

Assuming constant refrigerant properties in the transition elements of an elemental heat exchanger model results in excessive computation time and unconverged solutions. In addition, the capacity of the transition element is always either underpredicted or overpredicted by the constant property assumption. Although the capacity error is generally small (about 1% for the example shown), for tube-by-tube models with multiple circuits, the error in calculated capacity is potentially significant.

This paper proposes an algorithm to correct the transition element problems. The algorithm divides the transition element into single-phase and two-phase portions according to the available heat transfer in the first portion of the element. Appropriate single-phase and two-phase heat transfer equations are applied to each part so that the total capacity will not be miscalculated. The examples of condenser and evaporator simulations showed that the proposed algorithm is able to correct the transition element problems. With the proposed algorithm, the heat exchanger models correctly respond to the change of boundary conditions, eliminating the trap to the numerical solver caused by the constant-property assumption.

The transition element problem is more significant in the ε-NTU method than in the LMTD method. In the ε-NTU

method, both the refrigerant heat transfer coefficient and the effectiveness equation are affected by the transition element, but in the LMTD method, only the refrigerant heat transfer coefficient is affected. Although the proposed algorithm is designed for the ε-NTU method, it is also applicable to the LMTD method with a slight modification.

ACKNOWLEDGMENTS

The authors are thankful to the Oklahoma Center for the Advancement of Science and Technology (OCAST) and York International Unitary Products Group (a Johnson Controls Company) for their sponsorship of this project. Special thanks are due to Charles Obosu of York International UPG.

NOMENCLATURE

A	=	area, m^2
C	=	heat capacity rate, kW/K
F	=	heat exchanger correction factor
h	=	heat transfer coefficient, kW/m/K
i	=	enthalpy, kJ/kg/K
L	=	element length, m
LMTD	=	log mean temperature difference, °C
$\dot{m}$	=	mass flow rate, kg/h
NTU	=	number of transfer units
P	=	pressure, kPa
$\dot{Q}$	=	capacity, kW
r	=	ratio
R	=	thermal resistance, K/kW
T	=	temperature, °C
ΔT	=	temperature difference, °C
U	=	overall heat transfer coefficient, kW/m/K
$\dot{V}$	=	volumetric flow rate, m^3/min

Subscripts

1	=	first portion of transition element
air	=	air
c	=	cold fluid
fin	=	fin
h	=	hot fluid
in	=	inlet
liq	=	liquid phase
max	=	maximum
min	=	minimum
out	=	outlet
ref	=	refrigerant
s	=	surface
SP	=	single-phase
TP	=	two-phase
Tot	=	total element
tube	=	heat exchanger tube
vap	=	vapor phase

Greek Symbols

ε	=	effectiveness
η	=	efficiency
ϕ	=	relative humidity, %

REFERENCES

Dobson, M.K. 1994. Heat transfer and flow regimes during condensation in horizontal tubes. ACRC TR-57, Air-Conditioning and Refrigeration Center, University of Illinois at Urbana-Champaign.

Domanski, P.A. 1991. Simulation of an evaporator with non-uniform one-dimensional air distribution. *ASHRAE Transactions* 97(1):793–802.

Domanski, P., and D. Didion. 1983. Computer modeling of the vapor compression cycle with constant flow area expansion device. *Building Science Series 155*.

Ellison, R.D., F.A. Creswick, and W.L. Jackson. 1981. A computer model for air-cooled refrigerant condensers with specified refrigerant circuiting. *ASHRAE Transactions* 87(1):1106–24.

Fischer, S.K., C.K. Rice, and W.L. Jackson. 1998. The Oak Ridge heat pump model: Mark III version program documentation. ORNL/TM-10192, Oak Ridge National Laboratory, Oak Ridge, TN.

Gnielinski, V. 1976. New equation for heat and mass transfer in turbulent pipe and channel flow. *Int. Chem. Eng.* 16:359–68.

Harms, T.M., J.E. Braun, and E.A. Groll. 2004. The impact of modeling complexity and two-phase flow parameters on the accuracy of system modeling for unitary air conditioners. *HVAC&R Research* 10(1):5–20.

Heun, M.K., and W.E. Dunn. 1996. Principles of refrigerant circuiting with application to microchannel condensers: Part II—The pressure-drop effect and the cross-flow heat exchanger effect. *ASHRAE Transactions* 102(2):382–93.

Incropera, F.P., and D.P. DeWitt. 1996. *Introduction to Heat Transfer,* 3d ed., pp. 554–56. New York: John Wiley & Sons.

Iu, I., P.K. Bansal, P.K., S.J. Rees, D.E. Fisher, N.A. Weber, and J.D. Spitler. 2003. Energy efficiency analysis of a unitary heat pump system. *Proc. Int. Conf. on Building Systems and Facilities Management—Integrating Innovations and Technologies for a Built Environment, Singapore*, pp. 334–341.

Jiang, H., V. Aute, and R. Radermacher. 2002. A user-friendly simulation and optimization tool for design of coils. *Proc. of Int. Refrigerant Conf. at Purdue University.*

Kakac, S., and H. Liu. 2002. *Heat Exchangers: Selection, Rating, and Thermal Design*, 2d ed. Boca Raton, FL: CRC Press.

Kim, M.H., and C.W. Bullard. 2001. Development of a microchannel evaporator model for a CO_2 air-conditioning system. *Energy* 26:931–48.

Liang, S.Y., T.N. Wong, and G.K. Nathan. 2001. Numerical and experimental studies of refrigerant circuitry of evaporator coils. *Int. J. of Refrigeration* 24:823–33.

Liaw, J.S., M.S. Liu, C.Z. Wei, B.C. Yang, and C.C. Wang. 2002. Computer modeling for small air-conditioning systems capable of handling complex circuitry. *ASHRAE Transactions* 108(2):613–26.

Mullen, C.E., B.D. Bridges, K.J. Porter, G.W. Hahn, and C.W. Bullard. 1998. Development and validation of a room air-conditioning simulation model. *ASHRAE Transactions* 102(2):389–97.

Orth, L.A., D.C. Zietlow, and C.O.Pedersen. 1995. Predicting refrigerant inventory of R-134A in air-cooled condensers. *ASHRAE Transactions* 101(1):1367–75.

Paliwoda, A. 1992. Generalized method of pressure drop calculation across pipe components containing two-phase flow of refrigerants. *Int. J. of Refrigeration* 15(2):119–25.

Ragazzi, F., and C.O. Pedersen. 1991. Modular-based computer simulation of an air-cooled condenser. ACRC Technical Report ACRC TR-07, Air-Conditioning and Refrigeration Center, University of Illinois, Urbana-IL.

Schmidt, ThE. 1949. Heat transfer calculations for extended surfaces. *Refrig. Eng*., pp. 351–57.

Shah, R., A.G. Alleyne, and C.K. Bullard. 2004. Dynamic modeling and control of multi-evaporator air-conditioning systems. *ASHRAE Transactions* 110(1):109–19.

Souza, A.L., J.C. Chato, J.P. Wattelet, and B.R. Christoffersen. 1993. Pressure drop during two-phase flow of pure refrigerants and refrigerant-oil mixtures in horizontal smooth tubes. *Proceedings of the National Heat Transfer Conference* 243:35–41. American Society of Mechanical Engineering, Heat Transfer Division.

Vardhan, A., and P.L. Dhar. 1998. A new procedure for performance prediction of air conditioning coils. *Int. J. of Refrigeration* 21(1):77–83.

Wang, C.C., C.J. Lee, C.T. Chang, and S.P. Lin. 1999. Heat transfer and friction correlation for compact louvered fin-and-tube heat exchangers. *Int. J. of Heat and Mass Transfer* 42:1945–56.

Wattelet, J.P. 1990. Heat transfer flow regimes of refrigerants in a horizontal-tube evaporator. ACRC technical report, TR-55. Air-Conditioning and Refrigeration Center, University of Illinois at Urbana-Champaign.